Hindawi
Advances in Materials Science and Engineering
Volume 2022, Article ID 2661311, 8 pages
https://doi.org/10.1155/2022/2661311

*Research Article*

# Effects of Pit-Bottom-Soil Reinforcement on the Deformation of Subway Deep Foundation Pits Based on an Improved Model

**Yan Wang and Fei Zhang**

*Fujian Jiangxia University, Fuzhou, China*

Correspondence should be addressed to Fei Zhang; 2015034@fjjxu.edu.cn

Received 13 August 2021; Revised 19 November 2021; Accepted 23 March 2022; Published 27 April 2022

Academic Editor: Zhengyang Song



Reinforcement of pit bottom soil has been utilized in subway deep foundation-pit engineering in soft-soil areas. This study proposes an improved foundation-pit excavation model to better investigate the effect of soil reinforcement at the bottom of a pit on the deformation of a subway's deep foundation pits. The strength parameters of the reinforced soil utilized in the improved model could be obtained through a cone penetration test before and after the pit-bottom-soil reinforcement. The results show that the enveloped structure's lateral displacement and the surface settlement outside the pit were reduced by 37% and 23% after soil reinforcement, respectively. The uplift suppression in the centre of the base exhibited a significant effect, and the uplift suppression exceeded approximately 50%. Thus, the foundation reinforcement could effectively reduce the subway foundation-pit support structure's horizontal deformation, ground settlement, and the pit bottom soil's uplift deformation. The bending moment of the diaphragm wall was mainly affected near the excavation surface at the bottom of the pit. The closer the support position to the surface, the smaller the effect on the axial force.

## 1. Introduction

To construct foundation pits in a soft-soil area, foundation-pit excavation inevitably produces a large deformation due to the excavation unloading and construction load, which could significantly affect the foundation pit's stability and the surrounding environment's safety if not properly controlled [1–5]. Reinforcement of pit bottom soil has been gradually utilized in subway deep foundation-pit engineering in soft-soil areas. Many engineering applications have shown that the strength of soft-soil foundations could be effectively improved by reinforcing the pit bottom soil [6–10]. Therefore, it is necessary to systematically investigate the effect of soil reinforcement at the bottom of a pit on the deformation of a subway's deep foundation pits.

So far, researches on the reinforcement of the pit bottom soil mainly focus on numerical simulation adopting different reinforcement measures. Tan et al. [11] numerically simulated the internal force and deformation of foundation pits with full reinforcement at the bottom of the pits and proposed a reasonable cement-mixing ratio. Kang et al. [12] numerically analysed the influence of Mantang and skirt reinforcement on foundation-pit deformation and compared the two reinforcement measures. The excessive increase in the secant modulus of reinforced soil has little effect on controlling foundation-pit deformation. Yang et al. [13] investigated the influence of different pit-bottom reinforcement measures on the overall stability of foundation pits based on a two-dimensional numerical model. They analysed the sensitivity degree of different factors influencing the mechanical parameters of reinforced soil. The internal friction angle is the main factor affecting foundation-pit deformation. Zhu et al. [14] suggested that the triaxial mixing-pile reinforcement of the foundation-pit bottom could effectively reduce the lateral deformation of the diaphragm wall and the surface settlement outside the pit. Later, some researchers studied the effect of foundation soil reinforcement by combining the actual engineering reinforcement and measured deformation. Xia et al. [15] performed numerically simulated an actual foundation-pit

project and suggested that the grouting reinforcement at the bottom of foundation pits in a soft-soil area could effectively inhibit the lateral deformation of the diaphragm wall. Liu et al. [16] simulated the excavation deformation of the foundation-pit project of Xianghu station on Hangzhou Metro Line 1 and investigated the influence of the rate of replacement of the pit bottom reinforcement on the safety of the subway foundation pit and compared the measured data. However, the physical and mechanical parameters of the reinforced soil in the abovementioned study were mainly obtained from empirical values [17, 18]. The field-reinforced soil was not measured on-site, and the value of the actual reinforced soil was not obtained.

In practice, the quality of pit-bottom-soil reinforcement is considerably affected by the construction quality, and its mechanical properties become more complicated after the soil is disturbed by the reinforcement. Therefore, numerical analyses based on empirical values would differ from the actual situation. Many researchers paid attention to the risk assessment of the excavation system and foundation pits in recent years and attempted to mitigate risk and reduce accident occurrence [19–22]. However, the relevant researches at present are scarce. In this study, an improved model is proposed to simulate the foundation-pit excavation. Combined with the deep foundation-pit project of a subway station on Metro Line 6 in Fuzhou city, the cone penetration test (CPT) was conducted to measure the cone-tip resistance before and after the pit-bottom-soil reinforcement. The strength parameters of the reinforced soil were then obtained and utilized in the improved model. Then, the deformation of foundation-pit engineering for reinforced and unreinforced pit bottom soil was investigated. The analysed results could provide a scientific basis for soft-soil foundation reinforcement.

## 2. An Improved Model

*2.1. Model Establishment.* In order to consider the effect of the quality of pit-bottom-soil reinforcement affected by the construction quality and the mechanical properties after being disturbed by the reinforcement comprehensively, an improved finite element numerical model was suggested. The model could be established for the plane strain analysis since the shape and stress form of the foundation pit in the standard section are relatively regular. The Mohr–Coulomb constitutive model adopts the nonassociated flow rule in the calculation process, which could better solve the convergence problem under the action of ultimate bearing capacity. Thus, it could ensure the accuracy of the numerical analysis results. As for the displacement constraints, the left and right boundaries adopted horizontal displacement constraints. Horizontal and vertical constraints were set at the bottom, and free boundaries were set at the upper surface. In addition, the linear elastic constitutive model was adopted for the diaphragm wall and internal support. Furthermore, the Coulomb friction contact model was utilized to contact the diaphragm wall and the soil. The calculation flow of the improved model is shown in Figure 1.

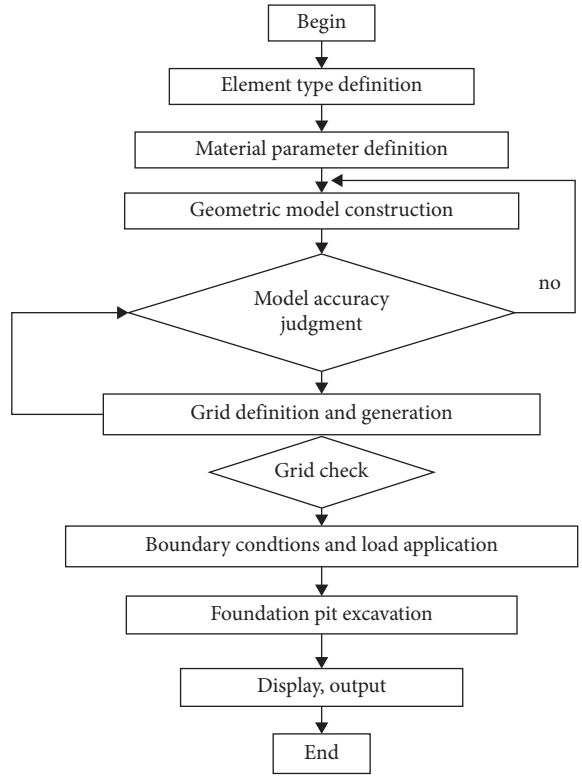


Figure 1: Calculation flow chart.

*2.2. Acquisition of Strength Parameters of Soil.* Notably, the values of strength parameters of the soil before and after the pit-bottom-soil reinforcement, such as the cone-tip and side-friction resistance, are crucial to the accuracy of the analysed results. The soil properties changed after the soft-soil foundation was strengthened through the cement-mixing method. However, evaluating its strength characteristics via conventional tests was difficult [23–26]. CPT is widely used in geotechnical engineering investigation as a common in situ test due to its simple equipment and reliable data. Recently, CPT has been used to investigate reinforced soil [18, 27–29]. Several empirical equations related to compressive strength and cone-tip resistance have also been established. For instance, Zhong [30] established a linear relationship model between cone-tip resistance ($q_c$) and unconfined compressive strength ($F_{cu}$) through a comparative analysis of field and laboratory tests. The relationship is expressed as follows:

$$F_{\mathrm{cu}} = aq_c + b, \tag{1}$$

where a and $b$ both are linear relation parameters. The cone-tip resistance of the cement-soil system measured via CPT could be conveniently converted into unconfined compressive strength. Thus, the strength characteristics of the cement-soil system could be determined.

In practical engineering, the secant deformation modulus ($E_{50}$) of a cement-soil system is usually utilized as its elastic modulus. Huang and Gao [31] proposed a linear relationship between the secant modulus and unconfined compressive strength of cement-soil systems listed as follows:

$$E_{50} = 126q_u. \quad (2)$$

The reinforced foundation is calculated according to the composite foundation as follows:

$$E_{sp} = mE_p + (1 - m)E_s, \quad (3)$$

where $E_{sp}$ is the modulus of the composite soil, $E_p$ and $E_s$ are the moduli of the pile body and the soil between the piles, respectively, and $m$ is the area replacement rate of the composite soil.

The effective internal friction angle and cohesion of the cement-soil system refer to the relevant regulations presented by Gong [32] in the "Foundation Treatment Manual". Then, the nonlateral compressive strength $F_{cu}$ of the cement-soil system is between 0.30 and 4.0 MPa, and its cohesion $c$ generally ranges from 20% to 30% of the $F_{cu}$. In addition, the internal friction angle varies between 20° and 30°. Considering the cement-soil discreteness in practical engineering, $c$ is adopted as 20% of the $F_{cu}$.

*2.3. Cone Penetration Test.* In practical engineering, the YJ-15 hydraulic press with a ZGS15-3 double-bridge probe is usually used for the penetration system of the static cone penetration to obtain the parameter values. However, the acquisition system could adopt an LMC-D310 static penetration microcomputer which has better sensitivity. Before testing, the probe should be calibrated according to the requirements of TBJ-93 (technical specification for CPT). The CPT test is performed on the soil at the test site to evaluate the cone-tip resistance of the undisturbed soil after completing the construction of the diaphragm wall and before reinforcing the soil at the bottom of the pit. Subsequently, the test should be repeated for the strip reinforcement belt in the foundation pit 90 days after soil reinforcement at the bottom of the pit to evaluate the cone-tip resistance of the cement-soil system.

## 3. Engineering Project

*3.1. Project Introduction.* The main foundation pit of the subway station is 290 m long and was constructed through the open-and-cover excavation process. The safety grade of the foundation pit is Class I [33, 34]. The retaining structure adopts the diaphragm wall and internal support form. The standard section of the main foundation pit was ~20 m wide, and the excavation depth was 18.5 m. The diaphragm wall was 800 mm thick. The used concrete adopted C40 (compressive strength 40 MPa), and the embedded depth was 26.6 m. In addition, four supports were set along the depth direction. The first support was reinforced concrete support, and the others were Φ609 steel supports (Q235 B steel) with 16 mm-thick walls. The relevant mechanical property parameters of concrete diaphragm wall and steel are listed in Table 1. The vertical spacing of each support was 0.8, 5.36, 4, and 4.5 m, respectively. Furthermore, the foundation pit soil was excavated in layers and blocks. The excavation depth of the five soil layers was 1.3, 5.36, 4, 4.5, and 3.35 m, respectively. Figure 2 shows the section of the foundation-pit-supporting structure in the middle standard section.

Table 1: Mechanical property parameters.

| Materials | $E$ (GPa) | $\nu$ |
|---|---|---|
| Concrete diaphragm wall | 30 | 0.2 |
| Concrete support | 30 | 0.2 |
| Steel support | 210 | 0.3 |

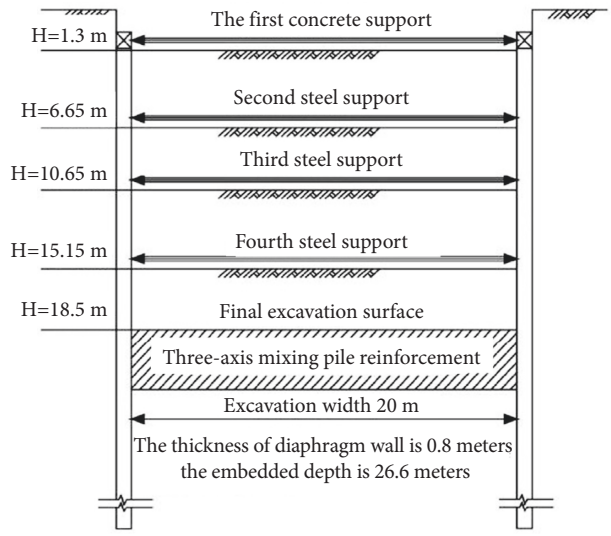


Figure 2: Sectional view of the foundation pit's support structure in a standard section.

*3.2. Engineering Geology.* According to the survey report, the rock and soil layers of the proposed site mainly include a quaternary artificial fill layer (including miscellaneous and rock fillings), marine sedimentary silt, muddy soil, silt mixed with sand (including mud), medium sand, silty clay layer, Jurassic tuff weathered rock, and bedrock. The site has multiple layers of groundwater. The station floor is located in the silt soil layer; hence, Φ850 @ 600 triaxial mixing piles with a 3-m width, 3-m depth, and 3-m spacing were adopted to reinforce the pit bottom within the standard section of the foundation pit after completing the construction of the diaphragm wall and before the excavation of the foundation pit to reduce the displacement of the retaining structure during the excavation of the foundation pit and improve the soil properties of the stratum at the location of the station floor. The soil reinforced with triaxial mixing piles comprised 42.5 cement with a water-cement ratio of 1.5 and 20% cement content. The unconfined compressive strength of the reinforced soil must exceed 1.0 MPa in 28 days.

## 4. Effect of Reinforcement on the Deformation of the Deep Foundation Pit after Excavating the Foundation Pit

The strength parameters of the cement-soil system were obtained from the CPT results (listed in Table 2, Table 3, and Table 4). The data presented in Table 3 are the

Table 2: Values of the linear relationship parameters.

| Soil layer | a | b |
|---|---|---|
| Muddy soil | 0.2131 | 0.0583 |

Table 3: Mechanical parameters of soil in the static penetration test.

| Geotechnical name | Taper tip resistance $q_c$ (MPa) | Side friction $f_s$ (kPa) | Friction ratio (%) | Cone-tip ratio penetration resistance $P_s$ (MPa) |
|---|---|---|---|---|
| Miscellaneous fill | 0.00 | 0.04 | - | - |
| Muddy soil | 0.42 | 6.79 | 16.17 | 0.46 |
| Silt and sand | 0.98 | 14.37 | 14.66 | 1.08 |
| Silt and sand | 1.06 | 16.03 | 15.12 | 1.17 |
| Silty clay | 2.00 | 27.40 | 13.70 | 2.20 |
| Coarse medium sand | 4.90 | 8.10 | 1.65 | 5.39 |
| Cement-soil | 5.7 | 89.1 | 15.47 | 5.61 |

*Note.* CPT was used to perform diversion hole construction in miscellaneous fill; hence, no data of this soil layer were obtained.

Table 4: Mechanical parameters of the soil layer.

| Name of the soil layer | Thickness (m) | $\gamma$ (kN•m$^{-3}$) | C (kPa) | Φ (°) | $E$ (MPa) | $v$ |
|---|---|---|---|---|---|---|
| Miscellaneous fill | 3.5 | 18 | 6 | 12 | 6.5 | 0.2 |
| Muddy soil | 2.5 | 16.5 | 10.3 | 7.7 | 8.9 | 0.46 |
| Silt and sand | 14.6 | 15.9 | 11.9 | 9.8 | 25.9 | 0.43 |
| Silt and sand | 7.4 | 16.0 | 13 | 10.5 | 12.4 | 0.39 |
| Silty clay | 2.6 | 19.7 | 30.4 | 17.4 | 40 | 0.31 |
| Coarse medium sand | 4.9 | 18.5 | 3 | 30 | 70 | 0.31 |
| Composite soil | 3 | 18 | 133 | 15 | 93 | 0.4 |

weighted average values of the cone-tip and side-friction resistance for each soil layer thickness. Table 4 lists the physical and mechanical parameters of each soil layer along with the mechanical parameters of the reinforced soil.

The deformation of the subway deep foundation pit with and without reinforcement after the foundation-pit excavation was further analysed through numerical simulations. The results were then compared with the measured data, providing a scientific basis for the deep foundation-pit reinforcement in soft-soil areas.

The step procedures of the numerical model are as follows: basic hypothesis (all layers of rock and Earth mass considered as an ideal elastoplastic body) ⟶ selection on parameters of numerical analysis model⟶ establishment of model and division of calculation grid ⟶ coordinate system and boundary conditions used for calculation. A 2D finite element numerical model was established for the plane strain analysis based on ABAQUS finite element software because the shape and stress form of the foundation pit in the standard section are regular. The plane size of the model was 140 m (length) × 90 m (depth). Both the soil and the diaphragm wall adopted an eight-node plane-strain reduction integration element (CPE8R). The internal support adopted a two-node plane linear beam element (B21). Horizontal displacement constraints were set at the left and right boundaries. Horizontal and vertical constraints were set at the bottom, and free boundaries were set at the upper surface. The finite element meshing diagram is shown in Figure 3.

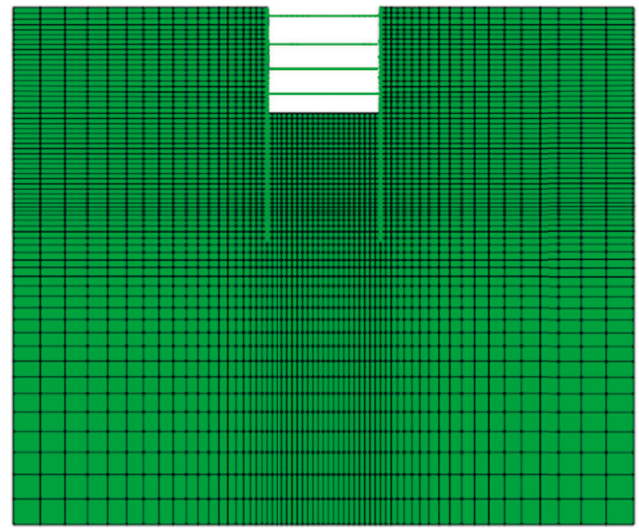

Figure 3: Finite element meshing diagram.

*4.1. Horizontal Displacement of the Wall.* Figure 4 presents the variation curve of the horizontal displacement of the diaphragm wall with depth and the bending-moment distribution diagram of the diaphragm wall with and without reinforcement. Figure 4(a) shows that the calculated horizontal displacements of the diaphragm wall after soil reinforcement in the passive area are consistent with the measured data, and the development trends are also consistent with these measured data. Therefore, the selection of the numerical calculation parameters is reasonable, and the

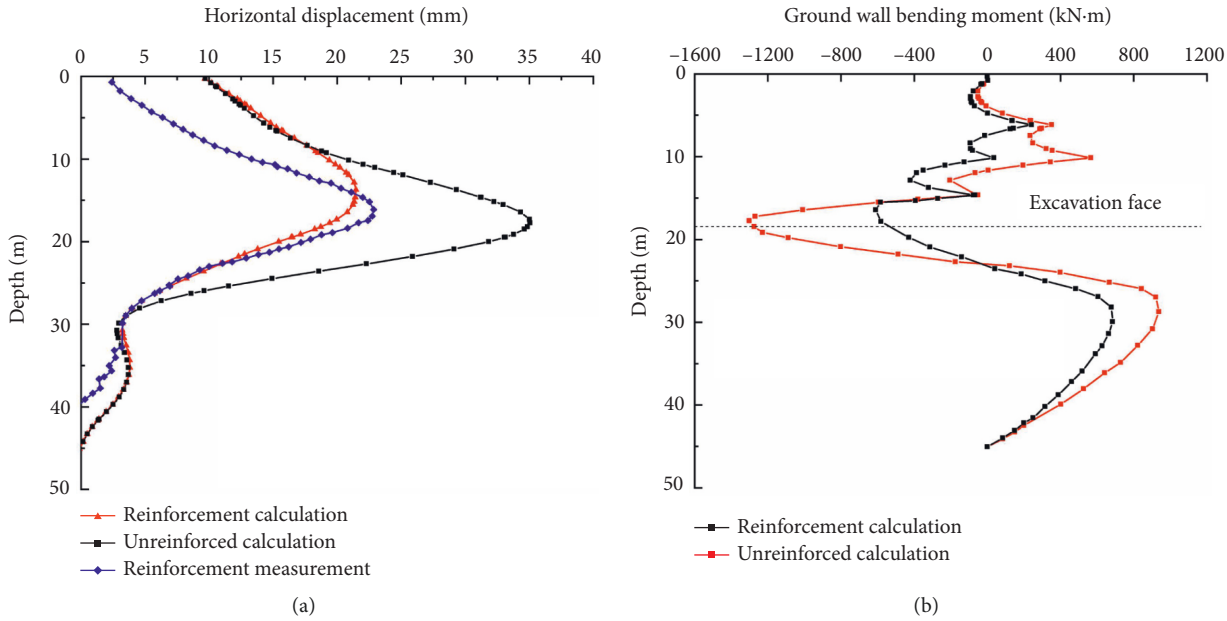


Figure 4: Horizontal displacement and bending-moment diagram of the diaphragm wall. (a) Horizontal displacement of the diaphragm wall. (b) Bending-moment diagram for the diaphragm wall.

cement-soil reinforcement effect could be well detected. The excavation deformation of the foundation pit can be predicted using the cone-tip resistance obtained via CPT.

Figure 4(a) also illustrates that the effect of soil reinforcement in the passive area on the lateral displacement of the diaphragm wall mainly occurs near the pit bottom. With and without reinforcement, the trends of the lateral deformation of the diaphragm wall were similar, and the lateral displacements near the pit bottom were different. The maximum lateral deformation of the diaphragm wall without reinforcement was 39.4 mm. The measured maximum lateral deformation of the diaphragm wall under reinforcement was 25 mm. Compared with the case of no reinforcement, the lateral deformation of the diaphragm wall after reinforcement was reduced by 37%. In addition, the position of the maximum lateral deformation moved upward. For the embedded retaining wall structure, the lateral deformation of the retaining structure is an important index for the environmental-impact control of the foundation pit. The safety protection grade of the subway station foundation pit was Grade I; thus, the maximum horizontal displacement of the retaining wall was $\leqq$0.2% H and $\leqq$30 mm, according to the technical regulations for deep foundation pits in Fujian Province. Compared with the maximum lateral deformation of the diaphragm wall under the two working conditions, the lateral deformation of the diaphragm wall prior to base reinforcement exceeded the value for deformation control. So, the lateral deformation of the diaphragm wall following base reinforcement was effectively controlled to fulfil the deformation-control requirements, indicating that soil reinforcement in passive areas of soft soil can effectively inhibit the lateral deformation of the diaphragm wall.

Figure 4(b) shows that following soil reinforcement in the passive area, the retaining structure's positive and negative bending moments were less than the bending moment in the case of no reinforcement. The maximum positive bending moment of the diaphragm wall was reduced from 947.64 kN m prior to reinforcement to 674.84 kN m postreinforcement, exhibiting a 29% decrease. The maximum positive bending moment was observed below the pit bottom. The maximum negative bending moment decreased from 1300.96 kN m prior to reinforcement to 620.09 kN m postreinforcement, exhibiting a decrease of 52%. The negative bending moment was located near the excavation surface above the pit bottom, which is consistent with the position of the maximum lateral deformation of the diaphragm wall. Compared with that prior to reinforcement, the maximum negative bending-moment position slightly moved up along the depth. The change in the bending-moment distribution diagram for the diaphragm wall before and after reinforcement shows that the effect of soil reinforcement on the internal force of the diaphragm wall in the passive area was prevalent near the excavation surface of the foundation pit. In addition, combined with the excavation conditions of the foundation pit, the sudden change in the bending moment of the diaphragm wall is consistent with the setting position of the support, which is also consistent with the results of previous studies [35, 36].

*4.2. Surface Subsidence.* Figure 5 shows the measured data and numerical analysis results of the external surface settlement of the foundation pit. The surface settlement was distributed in a groove manner. The settlement-influenced area was mainly located within the excavation depth range, two times from the diaphragm wall. The surface settlement converged at the position of the excavation depth, which was three times from the diaphragm wall. The measured

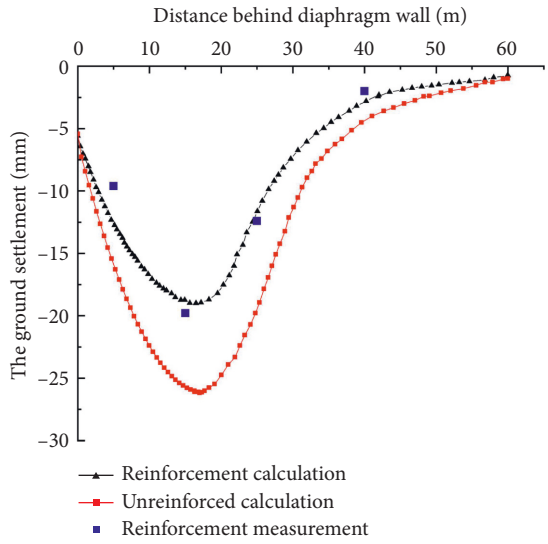


Figure 5: Curves of the ground settlement behind the wall.

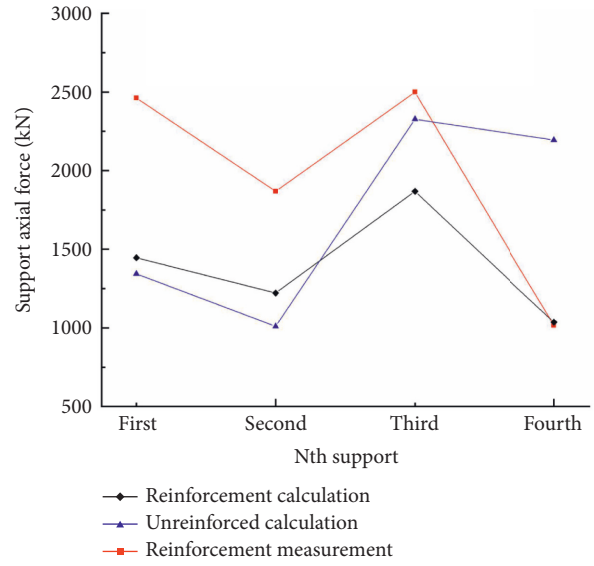


Figure 6: Axial forces of the inner support.

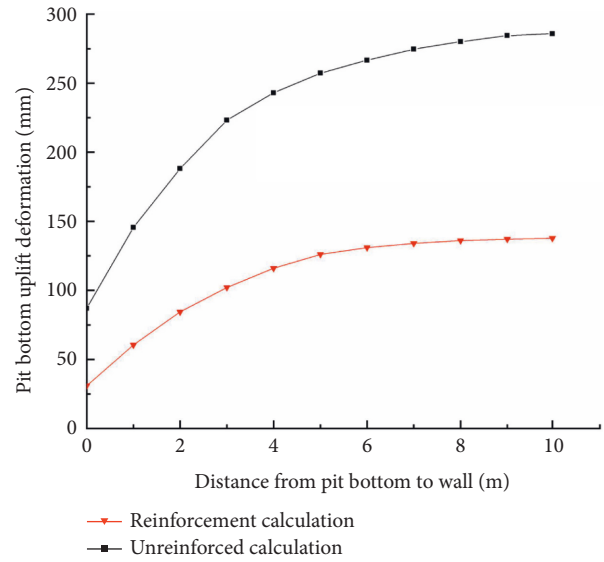


Figure 7: Calculated values of the foundation-pit rebound.

maximum settlement was −19.8 mm, which is slightly more significant than the numerical analysis result, and it was located at ~0.95 times the excavation depth. Compared with the calculated value, the location was closer to the retaining wall, but the changing trends of the two are the same.

A comparison of the surface settlement curves under the two working conditions showed that the surface settlement of the pit postsoil reinforcement in the passive area was less than that in the case of no reinforcement. Without reinforcement, the maximum surface settlement was −26 mm, which is too high and exceeds the design alarm value of −25 mm. The maximum measured settlement after reinforcement was −19.8 mm, which is ~23% lower than that without reinforcement. This shows that the soil reinforcement in the passive area of the soft-soil foundation pit affected the surface settlement of the pit, and its impact was not as significant on the lateral deformation of the diaphragm wall.

*4.3. Support Axis Force.* Figure 6 shows the change in each supporting axial force after complete foundation-pit excavation. The calculated supporting axial force trend is the same as that of the measured value even though the calculated and measured values are different. The measured axial force was more significant than the calculated value. The difference in the first supporting axial force was the largest. The main reason could be attributed to not considering the effect of factors, such as the foundation-pit excavation mode and site construction conditions, considerably affecting the axial force of the support in practice. Notably, the first support near the surface is easily affected by the ground construction load.

The axial force of each support did not exceed the design value before and after soil reinforcement at the bottom of the pit. Soil reinforcement in the passive area substantially affected the axial force of the two supports, particularly the bottom support. Without reinforcement, the axial force of the bottom support was 2194 kN, and the measured axial force after reinforcement was 1015.5 kN, demonstrating a 54% reduction. The analysis was conducted because the change in the axial force of the support is closely related to the deformation of the diaphragm wall. Soil reinforcement in the passive area effectively inhibited the lateral displacement of the diaphragm wall near the pit bottom, thereby substantially reducing the axial force of the support near the pit bottom.

*4.4. Foundation-Pit Bottom Uplift.* Figure 7 shows the uplift deformation of the bottom of the pit when the foundation pit was excavated to the bottom. Soil reinforcement in the passive area could reduce the uplift of the bottom of the pit, particularly the central range. For the unreinforced foundation pit, the uplift was 285.8 mm, whereas that after

reinforcement was 137.8 mm, exhibiting a decrease of more than 50%. Soil reinforcement in the passive area could thus effectively reduce the soil uplift at the bottom of the pit.

## 5. Conclusion

Adopting a subway deep foundation-pit project in Fuzhou as an example, we measured the cone-tip resistance before and after reinforcing the pit bottom soil via CPT. The strength parameters of the composite soil after reinforcing the cement-soil mixing piles were calculated. An improved model was suggested to analyse the effect of reinforcement on the deformation of the deep foundation pit after excavating the foundation pit compared with engineering measure results. The main conclusions are as follows.

(1) The strength parameters of the reinforced soil utilized in the improved model could be obtained through a cone penetration test before and after the pit-bottom-soil reinforcement. The improved model could be employed as a fast and effective method to investigate the effect of foundation reinforcement.

(2) The reinforcement of the pit bottom soil could effectively reduce the lateral deformation of the retaining structure, surface settlement outside the pit, and soil uplift at the bottom of the pit. After reinforcing the soil at the bottom of the pit, the maximum lateral deformation of the retaining structure was reduced by 37%, the maximum surface settlement outside the pit was reduced by 23%, and the maximum soil uplift deformation at the centre of the pit bottom was reduced by more than 50%.

(3) The reinforcement of the pit bottom soil reduced the bending moment of the diaphragm wall, and its influence range mainly occurs near the excavation surface of the foundation pit. Compared with other internal supports, soil reinforcement in the passive area significantly affected the axial force of the bottom support. The closer the support position to the surface, the smaller the effect on the axial force.

## Data Availability

The test data used to support the findings of this study are included within the article.

## Conflicts of Interest

The authors declare that they have no conflicts of interest regarding the publication of this paper.

## Acknowledgments

The authors acknowledge the Science Foundation of Fujian Jiangxia University (Grant nos. 19KTXZ02; JXZ2021007).

## References

[1] J. M. Xi and R. Q. Chen, "Deformation and surface settlement analysis of super-deep and large foundation pit excavation enclos," *Building Science*, vol. 36, no. 3, pp. 143–150, 2020.

[2] G. W. Clough and B. Schmidt, "Design and performance of excavations and tunnels in soft clay," in *Soft Clay Engineering*, E. W. Brand and R. P. Brenner, Eds., Elsevier, New York, NY, USA, pp. 569–634, 1981.

[3] Y. M. A. Hashash, H. Song, and A. Osouli, "Three-dimensional inverse analyses of a deep excavation in Chicago clays," *International Journal for Numerical and Analytical Methods in Geomechanics*, vol. 35, no. 9, pp. 1059–1075, 2011.

[4] Y. Sun, Y. Zhao, and D. Zhang, "Surface subsidence of pit-in-pit foundation in sand-cobble stratum in Beijing area," *Proceedings of the Institution of Civil Engineers - Ground Improvement*, vol. 172, no. 2, pp. 96–107, 2019.

[5] B. Li, "Comparison and selection of supporting schemes for foundation pit," *International Core Journal of Engineering*, vol. 5, no. 11, pp. 22–25, 2019.

[6] Q. Ma, S. Liu, and X. Fan, "A time series prediction model of foundation pit deformation based on empirical wavelet transform and NARX network," *Mathematics*, vol. 8, no. 9, p. 1535, 2020.

[7] B. Zhang, R. Jin, and X. L. Yu, "Analysis of foundation pit deformation monitoring results about xia shengou station in shenyang," *Advanced Materials Research*, vol. 2837, pp. 858–862, 2014.

[8] Q. W. Zhang, "Deformation analysis of deep foundation pit excavation under the effect of time and space," *Geotechnical Research*, vol. 7, no. 3, pp. 1–8, 2020.

[9] Z. Song, H. Konietzky, Y. Wu, K. Du, and X. Cai, "Mechanical behaviour of medium-grained sandstones exposed to differential cyclic loading (DCL) with distinct loading and unloading rates," *Journal of Rock Mechanics and Geotechnical Engineering*, 2020.

[10] J. Luo, R. Ren, and K. D. Guo, "The deformation monitoring of foundation pit by back propagation neural network and genetic algorithm and its application in geotechnical engineering," *PLoS One*, vol. 15, no. 7, Article ID e0233398, 2020.

[11] Z. Song, H. Konietzky, and M. Herbst, "Bonded-particle model-based simulation of artificial rock subjected to cyclic loading," *Acta Geotechnica*, vol. 14, no. 4, pp. 955–971, 2019.

[12] Z. J. Kang, Y. Tan, G. Deng, and B. Wei, "Impact of soil reinforcement in passive zone on the deformation behaviors of deep excavation," *Journal of Yangtze River Scientific Research Institute*, vol. 46, no. 5, pp. 118–123, 2020.

[13] B. Yang, Y. Tan, and C. J. Xv, "Influence of basal treatment patterns on deformation of deep excavation in soft ground," *Journal of Lanzhou University of Technology*, vol. 34, no. 6, pp. 119–123, 2017.

[14] Z. X. Zhu, S. W. Liu, X. R. Liu, and Y. Fu, "Study on the reinforcing effect of A deep foundation pit in soft soil of A Metro station," *Chinese Journal of Underground Space and Engineering*, vol. 10, no. 3, pp. 716–720, 2014.

[15] M. R. Xia, "Numerical simulation analysis of jet grouting effect of deep excavation bottom," *Journal of Civil & Environmental Engineering*, vol. 42, no. 1, pp. 64–69, 2020.

[16] X. Z. Liu, Y. S. Zhang, M. N. Gu, and H. Y. Zhuang, "Effects of reinforcement replacement rates at pit bottom on safety of

deep foundation pit of Xianghu Metro subway station in Hangzhou," *Chinese Journal of Geotechnical Engineering*, vol. 38, no. 298, pp. 136–142, 2016.

[17] S. Kim and R. J. Finno, "Inverse analysis of hypoplastic clay model for computing deformations caused by excavations," *Computers and Geotechnics*, vol. 122, no. 000, pp. 103499–104000, 2020.

[18] A. T. C. Goh, "Deterministic and reliability assessment of basal heave stability for braced excavations with jet grout base slab," *Engineering Geology*, vol. 218, pp. 63–69, 2017.

[19] S. S. Lin, S. L. Shen, A. N. Zhou, and Y. S. Xu, "Risk assessment and management of excavation system based on fuzzy set theory and machine learning methods," *Automation in Construction*, vol. 122, no. 4, Article ID 103490, 2021.

[20] K. Elbaz, S. L. Shen, Y. Tan, and W. C. Cheng, "Investigation into performance of deep excavation in sand covered karst: a case report," *Soils and Foundations*, vol. 58, no. 4, pp. 1042–1058, 2018.

[21] Q. Zheng, H. M. Lyu, A. N. Zhou, and S. L. Shen, "Risk assessment of geohazards along Cheng-Kun railway using fuzzy AHP incorporated into GIS," *Geomatics, Natural Hazards and Risk*, vol. 12, no. 1, pp. 1508–1531, 2021.

[22] S. S. Lin, S. L. Shen, A. N. Zhou, and Y. S. Xu, "Novel model for risk identification during karst excavation," *Reliability Engineering & System Safety*, vol. 58, Article ID 107435, 2021.

[23] P. J. Nussbaum and B. E. Colley, "Dam construction and facing with soil-cement," *Portland Cement Assoc R and D Lab Bull*, vol. 11, 1971.

[24] P. V. Sivapullaiah, J. P. Prashanth, A. Sridharan, and B. V. Narayana, "Technical Note Reactive silica and strength of fly ashes," *Geotechnical & Geological Engineering*, vol. 16, no. 3, pp. 239–250, 1988.

[25] L. V. . Doan, B. Lehane, and M. Cpt-Based, "Design method for axial capacities of drilled shafts and auger cast-in-place pile," *Journal of Geotechnical and Geoenvironmental Engineering*, vol. 147, no. 8, 2021.

[26] S. R. Kaniraj and V. G. Havanagi, "Compressive strength of cement stabilized fly ash-soil mixtures," *Cement and Concrete Research*, vol. 29, no. 5, pp. 673–677, 1999.

[27] L. N. Xu, L. Niu, T. Zhang, and Y. B. Wang, "Experimental researth on the unconfined compression strength characteristics of basalt fiberand cement stabilized riverbed silt," *Industrial Construction*, vol. 50, no. 2, pp. 109–112, 2020.

[28] W. G. Zhang, A. T. C. Goh, and F. Xuan, "A simple prediction model for wall deflection caused by braced excavation in clays," *J Computers and Geotechnics*, vol. 63, pp. 67–72, 2015.

[29] G. W. Li, S. Y. Wang, J. T. Wu, and Y. S. Zheng, "Damage control methods for detecting cement mixing piles by static cone penetration tests in reserved tubes," *Chinese Journal of Geotechnical Engineering*, vol. 41, no. 12, pp. 2215–2223, 2019.

[30] X. K. Zhong, *Research Onrapid Testing Methods of Cement-Soil Mixed Pile's Quality in Highway Project*, University of Technology, Guangzhou, China, 2013.

[31] S. M. Huang and D. Z. Gao, *Foundation and Underground Engineering in Soft Ground*, Architecture & Building Press, Beijing, China, 2nd edition, 2005.

[32] X. N. Gong, *Handbook of Ground Treatment*, Architecture & Building Press, Beijing, China, 2008.

[33] Ministry of Housing and Urban-Rural Development of the People's Republic of China, *Technical Code for Building Foundation Pit Support*, China Building Industry Press, JGJ120-2012, 2012.

[34] Fujian Provincial Department of Construction, *Technical Code for Building Foundation*, China Building Industry Press, DBJ13-07-2006, 2006.

[35] Y. H. Huang, J. Chen, W. H. Ke, and X. G. Huang, "Analysis of deformation of deep excavation in soft clay based on time-effect theory," *Journal of Yangtze River Scientific Research Institute*, vol. 34, no. 5, pp. 75–80, 2017.

[36] Y. G. Zhang, Y. L. Xie, Y. Zhang, J. B. Qiu, and S. X. Wu, "The adoption of deep neural network (DNN) to the prediction of soil liquefaction based on shear wave velocity," *Bulletin of Engineering Geology and the Environment*, vol. 80, no. 6, pp. 1–8, 2021.